Inorganic Chemistry

Article

pubs.acs.org/IC

Silica-Grafted 16-Electron Hydride Pincer Complexes of Iridium(III) and Their Soluble Analogues: Synthesis and Reactivity with CO

Martino Rimoldi and Antonio Mezzetti*

Department of Chemistry and Applied Biosciences, ETH Zürich, HCI H235, Zürich CH-8093, Switzerland

Supporting Information

ABSTRACT: The dihydride complexes [IrH_2(POCOP)] (**1a**) and [IrH_2(PCP)] (**1b**) (POCOP = 1,3-bis((di-*tert*-butylphosphino)oxy)-benzene; PCP = 1,3-bis((di-*tert*-butylphosphino)methyl)benzene) react with the surface silanols of mesoporous amorphous silica (SBA-15) to give H_2 and the silica-grafted, 16-electron iridium(III) monohydride species [IrH(O−SBA-15)(pincer)] (**2a** and **2b**). These materials contain a single iridium(III) species, that is a highly dispersed, coordinatively unsaturated siloxo hydride complex, as indicated by solid-state spectroscopic data. The siloxo complexes [IrH(^{i}Bu-POSS)(POCOP)] (**3a**) and [IrH(^{i}Bu-POSS)(PCP)] (**3b**) (^{i}Bu-POSS = $OSi_8O_{12}{}^iBu_7$) were prepared as soluble analogues of **2a** and **2b** to support their spectroscopic characterization. The coordinatively unsaturated, 16-electron species **2a** and **2b** react with CO to give the six-coordinate iridium(III) adducts [IrH(O−SBA-15)(CO)(POCOP)] (**7a**) and [IrH(O−SBA-15)(CO)(PCP)] (**7b**). Due to dissimilar electronic properties of the pincer ligands, **7a** undergoes reductive elimination of the silanol forming the Ir(I) complex [Ir(CO)(POCOP)] (**8a**), whereas **7b** is stable in oxidation state of III. The homogeneous siloxo carbonyl complexes [IrH(^{i}Bu-POSS)(CO)(POCOP)] (**9a**), [IrH(^{i}Bu-POSS)(CO)(PCP)] (**9b**), and [IrH($OSiMe_3$)(CO)(POCOP)] (**11a**) were prepared to substantiate the reactivity and the characterization of the silica grafted species.

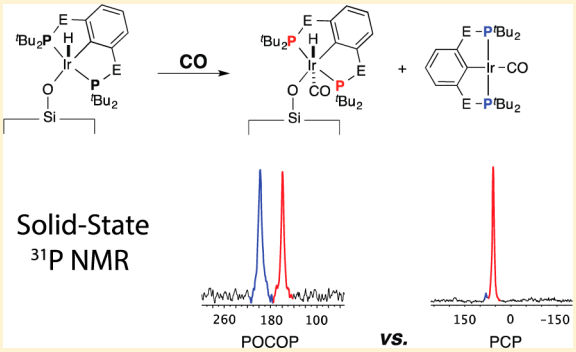

INTRODUCTION

In general, early transition metal complexes, in particular with d^0 metal ions, are the most explored silica-grafted species.[1−4] The successful combination of early transition metals and oxide supports is based on the high oxophilicity of hard metal ions such as zirconium(IV) and titanium(IV), whose complexes are stabilized by the interaction with the surface. In contrast, late transition metals have little affinity for oxygen-containing ligands, in particular when hydride ligands make the metal ion even softer.[5] A far-reaching consequence is that oxide-grafted, low-nuclearity complexes of late transition metals undergo aggregation to metal nanoparticles upon activation with H_2 or metal hydride formation.[6,7]

We have recently reported that the dihydride pincer complex [IrH_2(POCOP)] (**1a**)[8] (POCOP is 1,3-bis((di-*tert*-butylphosphino)oxy)benzene) reacts with amorphous mesoporous silica (SBA-15) to give the grafted hydrido siloxo complex [IrH (OSi ≡) (POCOP)] (**2a**).[9] The grafted complex **2a** gives a single set of ^{1}H and ^{31}P NMR signals, and the comparison of their chemical shifts with those of the soluble complexes [IrH($OSiMe_3$)(POCOP)] (**4a**) and [IrClH-(POCOP)] (**5a**) strongly suggests the presence of a single, coordinatively unsaturated 16-electron complex grafted to the silica surface via a single metal−siloxo bond. To corroborate this conclusion, we report herein [IrH(^{i}Bu-POSS)(POCOP)] (**3a**) (^{i}Bu-POSS = $OSi_8O_{12}{}^iBu_7$) (**3a**), a further homogeneous analogue of **2a**. To the best of our knowledge, the reaction of the dihydride complex [IrH_2(POCOP)] (**1a**) with the silanols of the silica surface to give the grafted complex [IrH(OSi≡)-(POCOP)] (**2a**) is the first of its class. Indeed, all other silica-grafted complexes (that is, involving a metal−OSi bond)[10] of late transition metals have been prepared from precursors that contain protolyzable ligands such as alkyl,[11−14] allyl,[15,16] amido,[17] siloxo,[18−20] acetylacetonato,[21] and hydroxo,[12,22,23] which readily react with the surface silanols upon elimination of the corresponding protonated species.

Also, [IrH (OSi≡)(POCOP)] (**2a**) is a rare example of a stable hydride complex of a late transition metal grafted on an oxide surface that catalyzes the hydrogenation of gaseous alkenes (ethene and propene) without decomposition. Indeed, it is recovered intact after the reaction and can be reused.[9] The large surface area and pore size, as well as the regular channel structure[24,25] of SBA-15, grant efficient diffusion of small molecules in the gas phase such as ethene and propene, which are rapidly hydrogenated by **2a**.[9] Herein, we extend the grafting approach to the iridium pincer complex [IrH_4(PCP)] (**6b**) (PCP is 1,3-bis((di-*tert*-butylphosphino)methyl)benzene) and report the synthesis of their homogeneous analogues. Furthermore, we describe the reaction of the hydride siloxo complexes with carbon monoxide and the tendency of the resulting Ir(III) carbonyl complexes to undergo reductive

Received: July 4, 2014
Published: October 27, 2014

   dx.doi.org/10.1021/ic501593k | *Inorg. Chem.* 2014, 53, 11974−11984

elimination of silanol. The latter study is of fundamental importance in view of the application of the silica-grafted hydrides because the reductive elimination of silanol, which may be triggered by any π-accepting ligands including alkenes, causes degrafting of the catalyst (and leaching in the case of liquid alkenes).

RESULTS AND DISCUSSION

Synthesis of 2a and of Its Soluble ^{i}Bu-POSS Analogue 3a. The silica-grafted complex [IrH(OSi≡)(POCOP)] (**2a**) used in this work was prepared according to the reported procedure (Scheme 1a)[9] with a loading of 13% and 21.2% (based on **1a**). Additionally, to check whether varying the hydroxyl group concentration on the surface may possibly affect the coordination sphere of the silica-grafted iridium complex, SBA-15 samples with different degrees of dehydroxylation were used (see Supporting Information). Irrespective of the pretreatment of SBA-15, all samples of **2a** showed solid-state ^{1}H and ^{31}P NMR spectroscopic fingerprint in agreement with those previously reported,[9] which, together with the points discussed below, supports a well-defined, 16-electron coordination environment for the iridium(III) ion of **2a**, in contrast with other grafted complexes, such as the bis(allyl) rhodium fragment on silica, whose podality varies with the extent of dehydroxylation of the silica.[26]

Scheme 1. Synthesis of the Silica-Grafted Iridium Hydride POCOP Pincer Complex 2a and of Its ^{i}Bu-POSS Analogue 3a

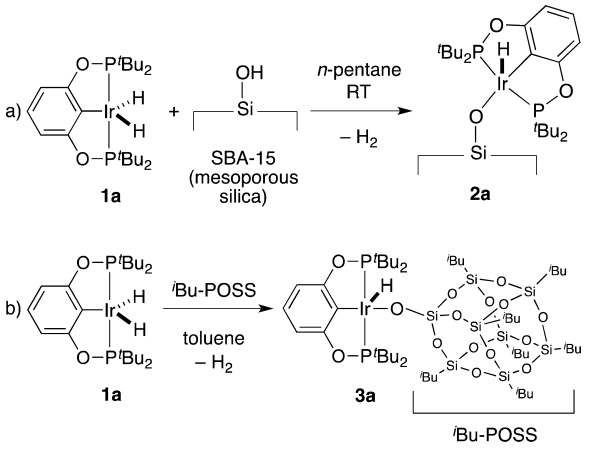

To substantiate that the Si−O−Ir-linkage in **2a** is formed by reaction of the dihydride complex **1a** with surface silanols, we studied the reactivity of [IrH$_2$(POCOP)] (**1a**) with polysilsesquioxanes, which have been widely explored as molecular models of the silica surface.[27−31] Upon treating dihydride **1a** with the 2-butyl-substituted monosilanolsilsesquioxane HO-Si$_8$O$_{12}$^{i}Bu$_7$ (^{i}Bu-POSS) in toluene, the color changed from red to orange. An excess of ^{i}Bu-POSS is required to reach complete conversion, but the resulting product contains unreacted ^{i}Bu-POSS. Analytically pure [IrH(OSi$_8$O$_{12}$^{i}Bu$_7$)(POCOP)] (**3a**) was obtained with a stoichiometric amount of ^{i}Bu-POSS by refluxing the reaction solution under static vacuum. The ^{31}P{^{1}H} NMR spectrum of the reaction solution shows the quantitative disappearance of the starting material **1a** and the formation of a single new species. The NMR data (^{31}P NMR δ 170.2, ^{1}H NMR δ −38.8, *p*-xylene-d_{10}) support the formulation of **3a** as the five-coordinate iridium(III) complex [IrH(OSi$_8$O$_{12}$^{i}Bu$_7$)(POCOP)] (Scheme 1b) with the same square-pyramidal structure and Ir−OSi linkage of the silica-grafted complex **2a**. The iridium(III) siloxo complex prepared with the ^{i}Bu-POSS molecule was isolated, characterized by ^{1}H, ^{31}P{^{1}H}, and ^{13}C{^{1}H} NMR spectroscopy (Supporting Information Figures S4−S13), and is indefinitely stable under inert atmosphere.

As shown in Figure 1, the ^{1}H and ^{31}P{^{1}H} NMR fingerprint of the ^{i}Bu-POSS complex [IrH(OSi$_8$O$_{12}$^{i}Bu$_7$)(POCOP)] (**3a**)

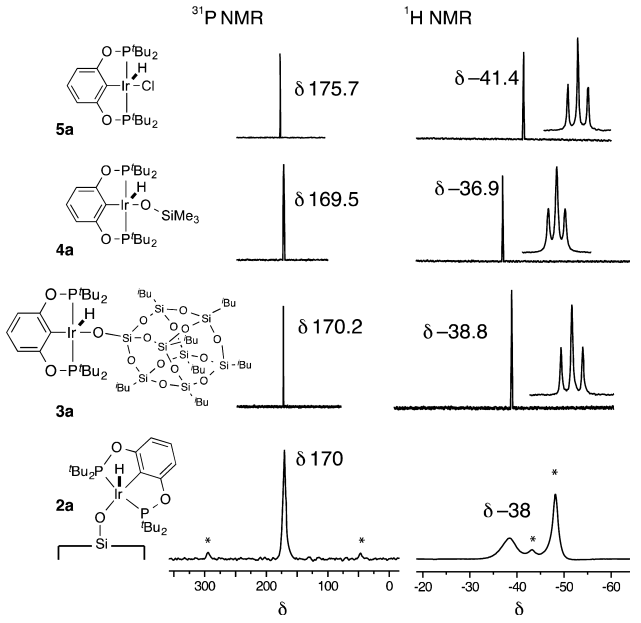

Figure 1. Solution (**3a**, **4a**, **5a**) (*p*-xylene-d_{10}) and solid-state (**2a**) ^{31}P and ^{1}H NMR spectra. Asterisks denote spinning side bands.

closely resembles those of the SBA-15-grafted complex **2a**, of the already reported siloxo complex [IrH(OSiMe$_3$)(POCOP)] (**4a**),[9] of [IrClH(POCOP)] (**5a**),[32] and of related square-pyramidal anilido complexes.[33,34] The high-field shift of the hydride signal is diagnostic of an apical hydride in a square-pyramidal geometry[34] for all these 16-electon Ir(III) complexes.

The ^{13}C NMR spectra (either in solution or in the solid state, Figure 2) further support the structural similarity of **2a**−**5a**. In particular, the two ^{13}C CP-MAS NMR resonances of the inequivalent quaternary *tert*-butyl C atoms at δ 39 and 42 are typical for all these complexes. The methyl groups are also inequivalent and should give two ^{13}C NMR signals, as observed in the solution NMR spectra of similar compounds, but the signals are not resolved in the solid-state ^{13}C CP-MAS NMR spectrum, which shows a single signal at δ 27. The aromatic carbon atoms resonate at δ 103, 108, 124, and 167, the latter signal being assigned to the *C*−O carbon atoms. The ^{13}C CP-MAS NMR of the chlorohydride derivative **5a**, which was measured for comparison, shows the same features (Figure 2).

The solid-state ^{1}H and ^{31}P NMR spectra of complex [IrH(OSiMe$_3$)(POCOP)] (**4a**)[9] reveal that the ^{31}P NMR signal of **4a** is split in two components at δ 168.5 and 170 (Supporting Information Figure S14). Similarly, the hydride gives two signals at δ −35.7 and −39.2, respectively, with a considerable difference in the chemical shifts (approximately 3.5 ppm, Supporting Information Figure S15). As the hydride resonates in solution (δ −36.9, *p*-xylene-d_{10}) at an intermediate chemical δ value of the two chemical shifts observed in the solid

dx.doi.org/10.1021/ic501593k | Inorg. Chem. 2014, 53, 11974−11984

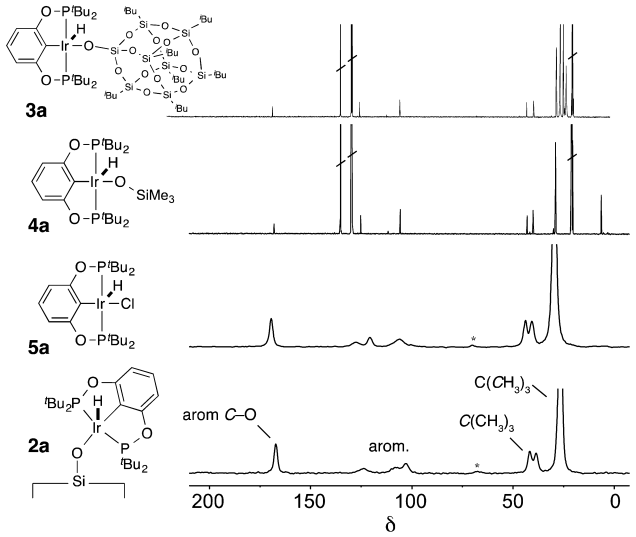

Figure 2. Solution $^{13}C\{^1H\}$ NMR spectra of **3a** and **4a**, and solid-state ^{13}C CP-MAS NMR spectra of **2a** and **5a**. The signals of the solvent (*p*-xylene-d_{10}) are striked through. Asterisks denote spinning side bands.

state, we tentatively explain the signal splitting with the occurrence of two different geometric isomers of **4a**, in which the $-OSiMe_3$ group points alternatively up or down respect to the pincer plane.[35] This would explain the solid-state splitting, whereas fast exchange at room temperature leads to a single averaged signal in the solution NMR spectra.

Overall, the spectroscopic data of **2a** and their comparison with those of **3a**, **4a**, and **5a** suggest that the first coordination sphere of the iridium(III) ion of **2a** is essentially the same as in the soluble analogues. In fact, both the ^{31}P and the ^1H NMR signals of **2a** indicate that a single five-coordinate species is present (or, at least, largely predominant) in the solid state. Species with a different coordination environment (podality) would feature significantly different ^{31}P and ^1H NMR chemical shifts. As six-coordinate POCOP hydride complexes of iridium(III) typically resonate at about δ 160,[34] the presence of such a species in significant amounts would give detectable signals different from that one at δ 170. Similar arguments apply for the ^1H NMR hydride signal, since a hydride chemical shift between δ −7 and −12 typically indicates a trans arrangement of the hydride and CO ligands in a six-coordinate iridium(III) complex.[34,36]

Therefore, the NMR spectroscopic data suggest that the constraints posed by the rigid pincer ligand are strong enough to maintain the iridium(III) ion in a well-defined first coordination sphere, that is, the pincer ligand, hydride, and siloxo. However, this does not imply that the complexes are embedded in a homogeneous and highly ordered environment such as that typical of a crystalline system, as will be discussed below for the IR data of the carbonyl derivative [IrH(O−SBA-15)(CO)(POCOP)] (**7a**).

H_2 Evolution from 1a + SBA-15. We have previously shown that, when SBA-15 is treated with the dihydride complex **1a** (in excess of the maximum loading of 21.2% w/w), the excess of reagent **1a** acts as scavenger for the dihydrogen formed and is converted to the tetrahydride complex **6a** (Scheme 2a).[9] Similarly, ^{i}Bu-POSS reacts with a stoichiometric amount of **1a** to give the soluble siloxo complex [IrH(OSi$_8$O$_{12}$^{i}Bu$_7$)(POCOP)] (**3a**), unreacted dihydride **1a**, and the tetrahydride complex **6a** (Scheme 2b), as indicated by the

Scheme 2. Synthetic Pathway for the H_2 Evolution During the Synthesis of 2a and 3a

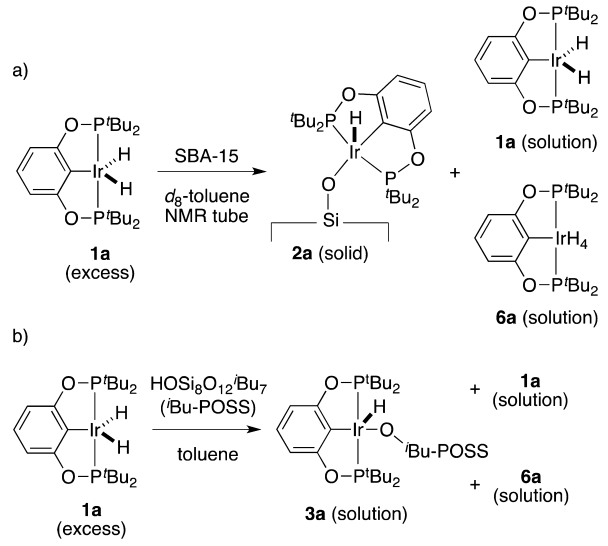

$^{31}P\{^1H\}$ and ^1H NMR spectra of the reaction solution (Figure 3). The integration of the ^1H and $^{31}P\{^1H\}$ NMR spectra is

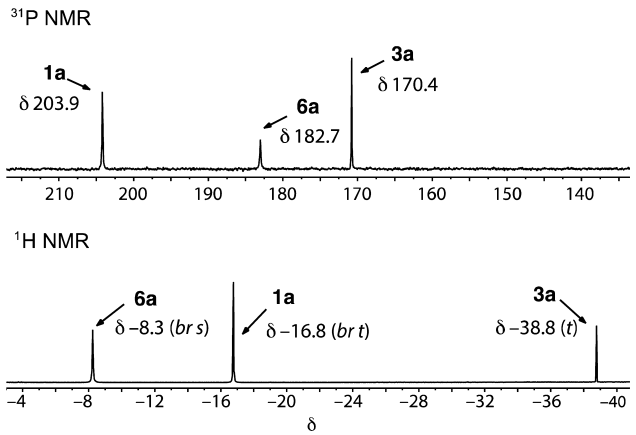

Figure 3. ^1H and $^{31}P\{^1H\}$ NMR spectra (toluene-d_8) of the reaction of **1a** with ^{i}Bu-POSS (Scheme 2).

consistent with the stoichiometry of the reaction showing a 1:1 ratio between the ^{i}Bu-POSS complex **3a** and the hydrogen trapped as **6a**. In contrast, when **1a** was treated with Et_3SiOH, the corresponding silanolate complex was not obtained, and only the starting complex **1a** was recovered.

Synthesis of PCP Complexes 2b and 3b. The synthetic approach was extended to the PCP series starting from the iridium hydride complex [IrH$_4$(PCP)] (**6b**), whose reaction with SBA-15 gave the silica-grafted species [IrH(O−SBA-15)(PCP)] (**2b**) (Scheme 3a), as indicated by its spectroscopic features. The solid-state ^{31}P NMR spectrum of **2b** contains a single signal at δ 66.5, whereas the hydride ligand resonates in the solid-state ^1H NMR at δ − 40.5 and gives a ν_{Ir-H} band at 2085 cm^{-1} in the FT-IR spectrum. A full spectroscopic characterization of **2b** is given in the Supporting Information (Figures S24−S27).

The spectroscopic data of the silica-grafted PCP derivative **2b** can be related to those of its soluble analogues as already done for its POCOP analogue **2a**, as five-coordinate square-pyramidal hydride PCP complexes give ^{31}P NMR signals

dx.doi.org/10.1021/ic501593k | Inorg. Chem. 2014, 53, 11974−11984

Scheme 3. Synthesis of the Silica-Grafted and ^{i}Bu-POSS Ir(III) Hydride PCP Complexes 2b and 3b

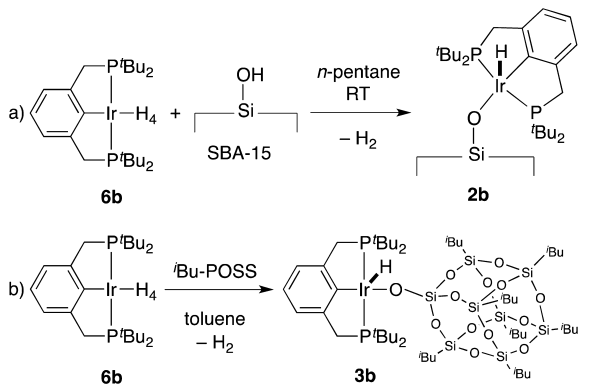

approximately in the range from δ 64 to 68. Thus, the $^{31}P\{^{1}H\}$ chemical shift of **2b** (δ 66.5) is close to those of square-pyramidal complexes such as [IrClH(PCP)][37] (**5b**) (δ 67.5) and, interestingly, to that of [IrH(OH)(PCP)][38] (δ 64.6). Similarly to the POCOP complexes, the ^{1}H NMR hydride chemical shift appears at a typically low frequency (δ −40.5, Figure 4).[37] The significance of the chemical shifts of the hydride ligands in these complexes is discussed below. The ^{13}C CP-MAS NMR spectrum of **2b** is compared with the $^{13}C\{^{1}H\}$ NMR spectrum of its soluble analogue [IrClH(PCP)] (**5b**) in Figure 5.

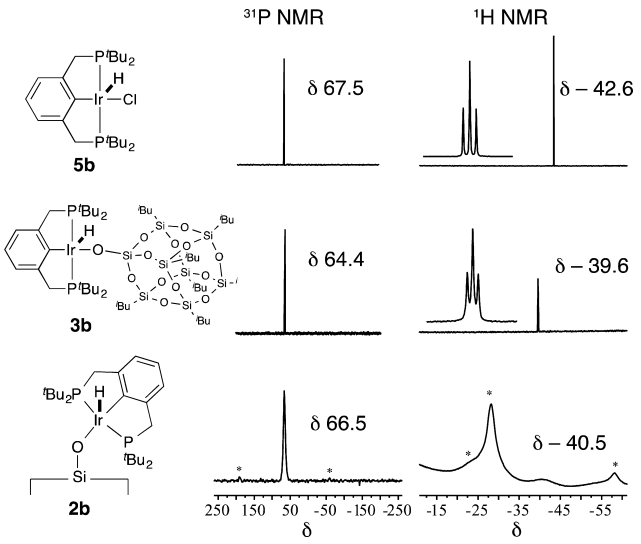

Figure 4. Solution (**3b**, **5b**) (toluene-d_8) and solid-state (**2b**) ^{31}P and ^{1}H NMR spectra. Asterisks denote spinning side bands.

A soluble analogue of **2b** was obtained by treating the iridium tetrahydride precursor **6b** with the 2-butyl-substituted mono-silanolsilsesquioxane $HOSi_8O_{12}{}^{i}Bu_7$ (^{i}Bu-POSS) (Scheme 3b). The ^{1}H, $^{13}C\{^{1}H\}$, and $^{31}P\{^{1}H\}$ NMR spectroscopic data of the resulting siloxo complex [IrH($OSi_8O_{12}{}^{i}Bu_7$)(PCP)] (**3b**) confirm its similarity with the silica-grafted compound **2b** and the chloro-hydride derivative **5b** (Figures 4 and 5).

To the best of our knowledge, the reaction of a hydride complex of a transition metal either with a soluble silanol or with the silanol groups of silica to give a fully characterized siloxo complex is unprecedented. However, silanols are known to react with main group hydrides of zinc,[39] gallium,[40] and aluminum[41] to give silanolate species. Also, some reactions of the Si−OH groups of silica with hydrides of main group and of actinide elements have been reported. Basset has described the reaction of dibutyltin dihydride with silica to give a material containing essentially one surface complex in which the tin atom is grafted via a metal-siloxo linkage. In this case, surface hydride complexes are possibly involved in the reaction as intermediates, but are not stable products.[42,43] Marks has prepared thorium(IV) hydride complexes supported on alumina, but the structure of the surface species was not discussed.[44] Besides being models for the silica-grafted species **2a** and **2b**, the soluble complexes **3a** and **3b** are rare examples of siloxo complexes of a late transition metal in general[45] and of iridium in particular.[46−52] A few siloxo iridium(I) species have been prepared by treating the appropriate iridium chloro complex with a silanolate salt[46,50] or by hydrolytic oxidation of a silane.[48,52]

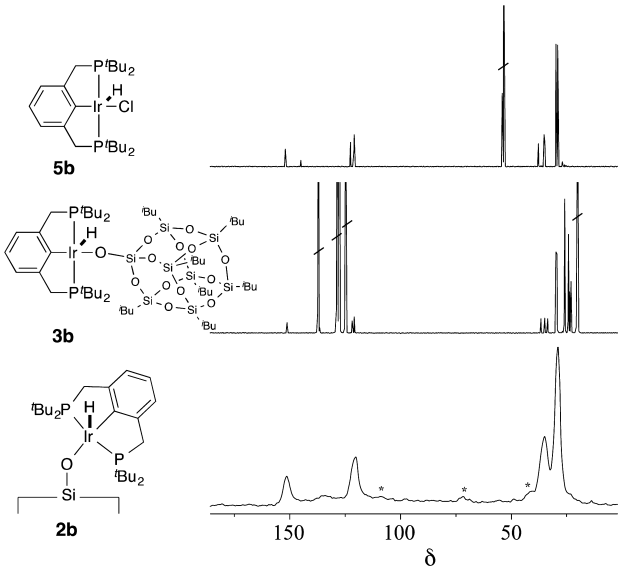

Figure 5. Solution (**3b**, **5b**) (toluene-d_8) and solid-state (**2b**) ^{13}C NMR spectra. Asterisks denote spinning side bands.

Donor Ability of Siloxo Ligands. Siloxo ligands are σ- and π-donors, and their overall donating ability is tuned by the electrophilicity of the metal. Therefore, they have been described as "sterically tunable pseudohalides".[53] Caulton has compared the donating ability of siloxo ligands to that of halides and of other anionic ligands in the d^6 complexes [RuH(X)(CO)($P^{t}BuMe)_2$] (X is a π-donating ligand such as halide, amide, OR, OPh, or siloxo),[54,55] which are isoelectronic with the iridium(III) hydrides **2**−**5**. The ν_{CO} frequencies suggest that the overall donating ability of X increases according to Cl < OPh < NHPh < OH < OCH_2CF_3 < $OSiPh_3$ < $OSiMe_3$.

As the iridium(III) siloxo complexes [IrH(X)(pincer)] (pincer = POCOP (**a**) or PCP (**b**); X = O−SBA-15, **2**; $OSi_8O_{12}{}^{i}Bu_7$ (^{i}Bu-POSS), **3**; $OSiMe_3$, **4**; Cl, **5**) do not contain a probe carbonyl ligand, we use here the ^{13}C NMR chemical shift of the *ipso*-carbon atom of the pincer ligand as an alternative probe of the overall donating ability of X to assess subtle structural changes within this series of otherwise analogous five-coordinate complexes (Table 1).[56] A downfield shift can be taken as an indication of an electron poor carbon atom, and hence of a more electron deficient metal center. The ^{13}C NMR chemical shifts of the *ipso*-C atom range for a total of

dx.doi.org/10.1021/ic501593k | Inorg. Chem. 2014, 53, 11974−11984

Table 1. ^{13}C NMR Chemical Shift ($\delta(^{13}C)$) of the *ipso* C Atom in [IrHX(pincer)]

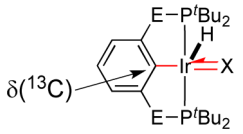

complex	E	X	$\delta(^{13}C)$	conditions
2a	O	O−SBA-15	108	solid state
4a	O	$OSiMe_3$	111.7	*p*-xylene-d_{10}
3a	O	^{i}Bu-POSS	112.5[a]	*p*-xylene-d_{10}
5a	O	Cl	118.5[b]	CD_2Cl_2
2b	C	O−SBA-15	134	solid state
3b	C	^{i}Bu-POSS	136.9[c]	toluene-d_8
5b	C	Cl	145.7[d,e]	toluene-d_8

[a]In toluene-d_8: δ 111.9. [b]Ref 32. [c]In *p*-xylene-d_{10}: δ 137.5. [d]This work, prepared according to ref 37. [e]In CD_2Cl_2: δ 144.9.

approximately 10 ppm from δ 108 (**2a**) to δ 118.5 (**5a**) in the POCOP series, and between δ 134 (**2b**) and δ 144.9 (**5b**) for the PCP complexes. The largest $\Delta\delta$ is that between the chloro hydride complexes [IrClH(pincer)] (**5**) and the siloxo derivatives **2**−**4**. Smaller δ differences are observed between the SBA-15-grafted species **2**, trimethylsiloxo complex **4**, and the ^{i}Bu-POSS analogue **3**.

We conclude that the overall ($\sigma + \pi$) donating ability of the siloxo ligand in the silica-grafted complexes **2** and in their ^{i}Bu-POSS and $OSiMe_3$ analogues **3** and **4** is very similar, and is significantly larger than that of the chloro ligand, in line with the trend found for [RuH(X)(CO)($P^tBuMe)_2$].[54,55] Although the σ and π contribution cannot be evaluated independently, it is reasonable to assume that both components are larger for the siloxo than for the chloro ligand. It should be noted that the π-donation from the silanolate ligand may contribute to the stabilization of the 16-electron siloxo complexes **2**−**4**, as generally observed for five-coordinate complexes of d^6 metal ions.[57−59]

Structural Considerations. As attempts to grow single crystals of X-ray quality failed, no structural information is available for the siloxo complexes **3** and **4**. However, ^{1}H NMR spectroscopic data are informative when compared with those of [IrClH(PCP)] (**5b**) and [IrH(OH)(PCP)], whose structures are known. Interestingly, the hydride ligand of the latter complex resonates approximately 12 ppm at lower field than **5b** (Table 2). The structure of the chlorohydride complex **5b** is perfectly square-pyramidal, as indicated by the C(aryl)−Ir−Cl (α) angle of 179.7(2)°.[60] As a difference, the α angle of the hydroxo (163.8(13)°)[38] and anilido (166.46(16)° and 164.49(9)°)[33] complexes indicates a distortion from this geometry that cannot be attributed to steric reasons, because the distortion trend does not follow the order of the steric requirements of the chloro and the hydroxo ligands. A possible electronic origin is discussed below and in the context of the carbonyl derivatives. Although steric effects cannot be excluded for the more bulky siloxo substituents, it is reasonable to assign an intermediate value of α, between 179° and 163° to the siloxo complexes.

Table 2. Hydride ^{1}H NMR Chemical Shifts and Distortion Angle α of [IrHX(pincer)]

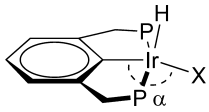

complex	X	$\delta(^1$H, Ir−H)	conditions	α (deg)
5b	Cl	−42.6	toluene-d_8[a]	179.7(2)[b]
2b	O−SBA-15	−40.5	solid state	
3b	^{i}Bu-POSS	−39.6	toluene-d_8	
	NHPh	−38.2	*p*-xylene-d_{10}[c]	165.5 (av)[d]
	OH	−31.0	cyclohexane-d_{12}[e]	163.8(13)[e]

[a]This work, prepared according to ref 37. [b]Ref 60. [c]Ref 33. [d]Of two crystallographically independent molecules, see ref 33. [e]Ref 38.

The effect of the nature and electronic properties of the ligands on the geometry of five-coordinate d^6 metal complexes has been discussed in detail.[61,62] σ-Donor ligands, such as hydride, open the L−M−L angle α trans to it, thus favoring a square-pyramidal geometry, whereas π donor ligands promote a geometric distortion in the opposite direction. With α = 179.7(2)°, [IrClH(PCP)] (**5b**) nicely fits in this trend. In the siloxo complexes (**3b**−**5b**), the effect of the π donating siloxo ligand adds to the effect of the σ donor (hydride), and the resulting effect cannot be assessed without calculation. However, the data summarized in Table 2 suggest that the square-planar structure distorts toward pseudo-trigonal-pyramidal (Y-shape) as the π-donating ability of X increases. The deviation from the square-pyramidal geometry is driven by the increasing π-donor ability of the X ligand, which causes a 4-electron π/π repulsion[59] with the occupied iridium d_{xy} orbital shown in Figure 6.

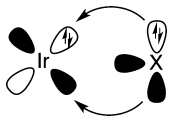

Figure 6. Schematic representation of the 4-electron π/π repulsion between iridium and a π-donating ligand.

The distortion toward the Y-shape minimizes this repulsion, and the structural rearrangement maximizes the dative π-bonding interaction between the X ligand and iridium. As the extreme high-field shift of the hydride signal is generally assigned to the presence of a vacant coordination site in the trans position,[34] it is reasonable to assume that the distortion toward Y-shape affects the hydride chemical shifts in the opposite direction. Although the hydroxo complex is not known in the POCOP series, a similar trend of the hydride NMR chemical shift of complexes **2a**, **3a**, and **5a** is observed (Figure 1).[9]

Reaction of 2a with CO. To confirm that the silica-grafted complex is a 16-electron, coordinatively unsaturated species, the silica-grafted complex **2a** was exposed to a CO atmosphere (1.5 bar absolute), whereupon the orange solid turned immediately white. Upon standing, the color changed to yellow (Supporting Information Figure S38). The ^{31}P NMR and IR spectra (Figure 7) indicate that the primary addition product is the six-coordinate, silica-grafted iridium(III) complex [IrH(OSi≡)(CO)(POCOP)] (**7a**), which then undergoes reductive elimination of silanol to give the known[8] iridium(I) species [Ir(CO)(POCOP)] (**8a**) (Scheme 4). The latter reaction reaches a conversion of ca. 60−70% after 15 h (by IR spectroscopy). Samples of **2a** with different loadings gave the same IR and NMR spectroscopic patterns.

dx.doi.org/10.1021/ic501593k | *Inorg. Chem.* 2014, 53, 11974−11984

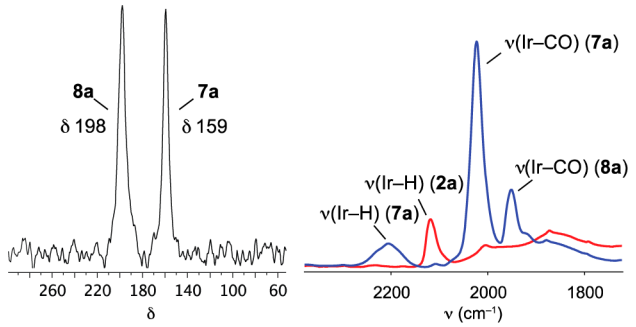

Figure 7. Solid-state ^{31}P MAS NMR and FT-IR spectrum of the reaction of **2a** with CO.

Scheme 4. Reaction of [IrH(O–SBA-15)(POCOP)] (2a) with CO

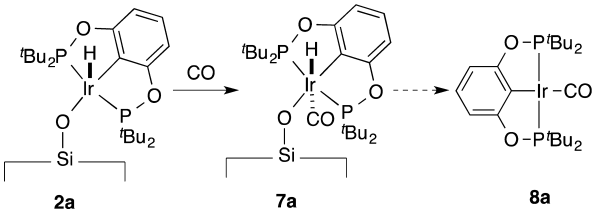

The solid-state ^{31}P MAS NMR spectrum of the reaction product shows a signal at δ 198 that is assigned to [Ir(CO)(POCOP)] (**8a**) (adsorbed on SBA-15) by comparison with the reported[8] ^{31}P NMR data (Figure 7, left). The additional signal at δ 159 is indicative of a six-coordinate pincer complex and is hence assigned to the silica grafted Ir(III) carbonyl complex **7a**.[34] In agreement, the ^{1}H MAS NMR spectrum of the solid exhibits a hydride signal at δ −7.5 (Supporting Information Figures S39 and S40), which indicates a *trans* arrangement of the hydride and CO ligands in a six-coordinate iridium(III) complex.[33] After washing the resulting solid with hexane and filtering off the white residue, the ^{31}P{^{1}H} NMR spectrum of the mother liquors showed a single signal corresponding to that of **8a**.[8] This is in agreement with the cleavage of the Ir–OSi bond upon reductive elimination and indicates that the resulting carbonyl complex is not chemically bonded to the surface.

The course of the reaction of **2a** with carbon monoxide was monitored by FT IR spectroscopy. In agreement with the ^{1}H and ^{31}P MAS NMR data, the IR spectra show that the reaction of **2a** with CO instantaneously forms the iridium(III) carbonyl complex [IrH(OSi≡)(CO)(POCOP)] (**7a**), whose ν_{IrH} and ν_{CO} bands appear at 2205 and 2026 cm^{-1}, respectively (Figure 7 right). With time, the silica-grafted iridium(III) carbonyl complex **7a** undergoes reductive elimination to [Ir(CO)(POCOP)] (**8a**) (ν_{CO} bands at 1952 and 1924 cm^{-1}, see Supporting Information).

The analysis of the IR spectra of the grafted species **7a** (and of its reductive elimination product **8a**) gives further insight into the interactions between the grafted complexes and the surface. In fact, the full widths at half-maximum (fwhm) of the carbonyl peaks of the grafted carbonyl species **7a** and of its product of reductive elimination of a silanol **8a** are 28 and 23 cm^{-1}, respectively. The latter species is physisorbed on the surface, from which it is extracted with toluene and unambiguously identified as [Ir(CO)(POCOP)] (**8a**) by solution NMR spectroscopy. The solid-state IR spectrum of crystalline **8a** shows a band with a fwhm of 15 cm^{-1}. Thus, a small difference exists between the observed fwhm values of surface and molecular compounds, which can be explained by the occurrence of weak interactions between the silanols of the intrinsically nonuniform silica surface and the carbonyl ligands (and hence with the second coordination sphere of the grafted complex).[63] This information complements that from the ^{31}P and ^{1}H NMR spectroscopic data of **2a** and **7a** (see discussed above),[64] which suggest a five-coordinate environment for (at least the great majority of) the metal ions. Overall, it can be concluded that the bulky and rigid pincer ligand maintains the reactive 16-electron iridium(III) in a controlled and uniform first coordination sphere, whereas the second coordination sphere of the complex interacts with the heterogeneous silica surface.

The ^{i}Bu-POSS and siloxo complexes [IrH(^{i}Bu-POSS)(POCOP)] (**3a**, ^{i}Bu-POSS is $OSi_8O_{12}{}^{i}Bu_7$) and [IrH(OSiMe$_3$)(POCOP)] (**4a**) were used as soluble analogues of the silica-grafted complex **2a** to reproduce its reactivity with CO in solution. Upon exposing [IrH(^{i}Bu-POSS)(POCOP)] (**3a**) to CO in toluene, the red solution became immediately colorless. The ^{31}P{^{1}H} NMR spectrum of the reaction solution shows the complete conversion of **3a** to a single new species that we formulate as [IrH($OSi_8O_{12}{}^{i}Bu_7$)(CO)(POCOP)] (**9a**) (Scheme 5). This is supported by the close similarity of its

Scheme 5. Reaction of [IrH(^{i}Bu-POSS)(POCOP)] (3a) with CO

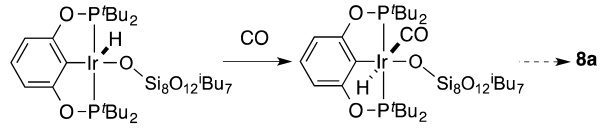

chemical shift (δ 159.7) with those of the grafted carbonyl complex **7a** (δ 159) and of [IrClH(CO)(POCOP)] (**10a**) (δ 161.8) (see Supporting Information). Furthermore, the hydride chemical shift of **9a** (δ −7.04, toluene-d_8) is close to those of the SBA-15-grafted Ir(III) carbonyl **7a** (δ −7.5, solid-state) and of **10a** (δ −8.16, *p*-xylene-d_{10}).

The Ir(III) ^{i}Bu-POSS carbonyl complex **9a** is not stable at room temperature and reductively eliminates the corresponding silanol to give [Ir(CO)(POCOP)] (**8a**) over time, as already observed for the silica-grafted analogue **7a** (Schemes 4 and 5). The trimethylsiloxo analogue [IrH(OSiMe$_3$)(CO)(POCOP)] (**11a**) has a more pronounced tendency to reductive elimination than **9a**. Indeed, upon exposure of [IrH(OSiMe$_3$)(POCOP)] (**4a**) to CO in *p*-xylene, the solution color turned immediately from red to deep yellow, and its ^{31}P{^{1}H} NMR spectrum showed the exclusive formation of [Ir(CO)(POCOP)] (**8a**), the reductive elimination product (Scheme 6). Instead, when a solid sample of **4a** was exposed to a CO atmosphere (1 bar abs), the color of the solid changed within 1 h from red to light yellow. After removal of CO, the IR spectrum (CsI) of the solid showed the presence of two ν_{CO} bands. The band at 1938 cm^{-1} is assigned to the iridium(I) carbonyl complex **8a**, and the second one at 2012 cm^{-1} to the iridium(III) siloxo carbonyl complex [IrH(OSiMe$_3$)(CO)(POCOP)] (**11a**) (Supporting Information Figure S45). A broad band at 2244 cm^{-1} is assigned to the iridium–hydride stretching vibration of the latter complex. Thus, it was possible

dx.doi.org/10.1021/ic501593k | *Inorg. Chem.* 2014, 53, 11974–11984

Scheme 6. Solution and Solid-State Reactions of [IrH(OSiMe$_3$)(POCOP)] (4a) with CO

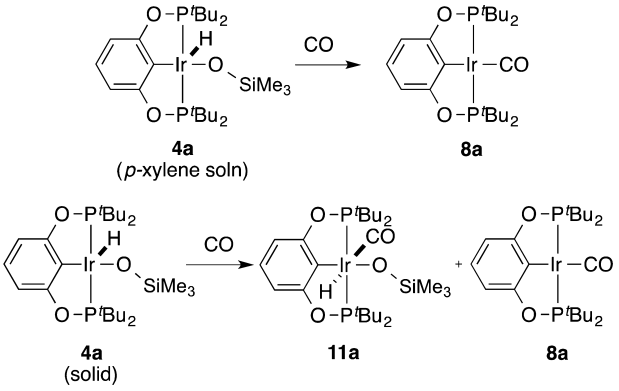

to convert **4a** to the carbonylated iridium(III) adduct **11a** avoiding the fast reductive elimination process that characterizes its reactivity in solution (Scheme 6).

Reactions of 2b and 3b with CO. The carbonylation reaction was performed also with the phosphine-based grafted pincer complex **2b** and the soluble species **3b**. In agreement with the observed reactivity of **2a**, the solid becomes white immediately after exposure to CO, affording the new species [IrH(O−SBA-15)(CO)(PCP)] (**7b**) (Scheme 7).

Scheme 7. Synthesis of [IrH(O−SBA-15)(CO)(PCP)] (7b) and [IrH(^{i}Bu-POSS)(CO)(PCP)] (9b)

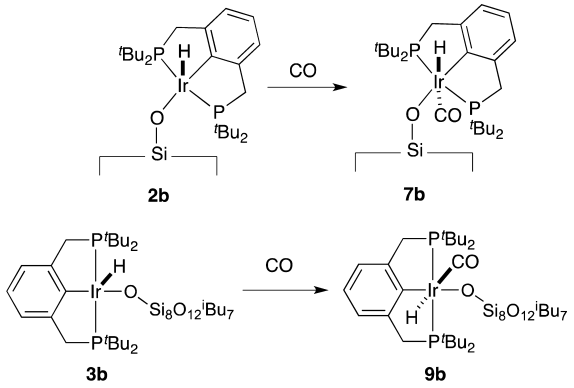

At difference with the POCOP derivative **7a**, which undergoes fast reductive elimination as indicated by the development of the yellow color, no further color change was observed over time, and the carbonyl adduct **7b** visually appeared to be stable. Accordingly, the solid-state ^{31}P NMR spectrum recorded immediately after the carbonylation reaction (Figure 8, top left) shows the formation of a single species with a chemical shift of δ 57.3. The signal of the corresponding reductive elimination product, the iridium(I) complex [Ir(CO)(PCP)] (**8b**), is hardly visible, indicating that only a negligible amount thereof is formed (see below). The observed chemical shift is characteristic of a six-coordinate phosphine-based iridium(III) complexes, such as for instance the complex [IrClH(CO)(PCP)] (**10b**), and supports the formulation of **7b** as the carbonylated product.[33,65]

In agreement with literature data,[33,65] the proton NMR spectrum of **7b** shows the signal for the hydride ligand at δ −6.9 (Supporting Information Figure S49). The solid-state ^{31}P NMR spectrum of the same sample of **7b** measured after 10 h

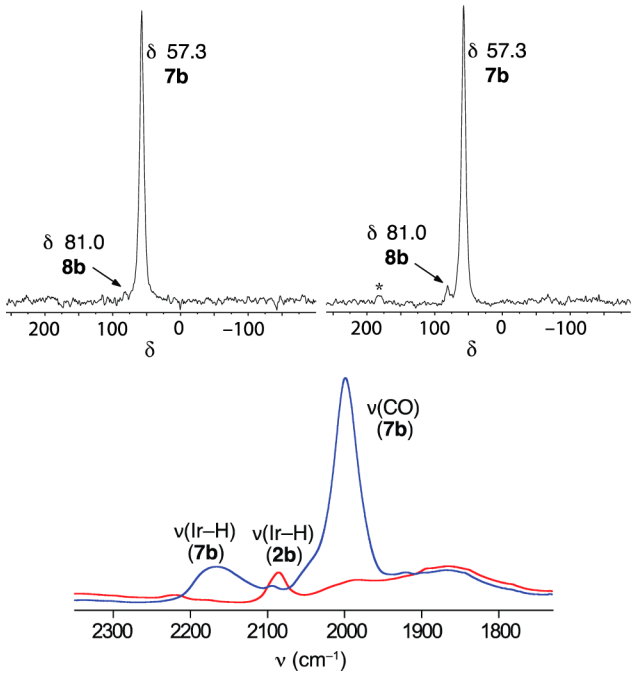

Figure 8. Solid-state ^{31}P MAS NMR spectra of [IrH(O−SBA-15)(CO)(POCOP)] (**7b**) immediately after the carbonylation reaction (top left) and after 10 h (top right), and FT-IR spectra of **2b** (bottom red) and of **7b** (bottom blue).

showed a weak signal corresponding to **8b** (Figure 8, top right). This indicated that the reductive elimination process occurs to a negligible extent for the silica-grafted PCP complex. The IR spectrum of **7b** is in agreement with the observations done by NMR spectroscopy. The newly appearing bands at 1999 and 2167 cm^{-1} are assigned to the carbonyl and hydride stretching, respectively, whereas the Ir−H band of the silica-grafted hydride complex **2b** has disappeared (Figure 8, bottom).

The ^{i}Bu-POSS complex **3b** readily reacts with CO in toluene solution. The resulting six-coordinate complex [IrH(^{i}Bu-POSS)(CO)(PCP)] (**9b**) is a molecular model of the grafted species **7b**. The ^{31}P{^{1}H} NMR shift at 56.9 and the ^{1}H hydride shift at −6.26 are in good agreement with the spectroscopic data of the grafted counterpart. Interestingly, the formation of the reductive elimination products [Ir(CO)(PCP)] (**8b**) was not observed even after a prolonged period in solution (Scheme 6), a fact again in agreement with the observed stability of the silica-grafted species **7b**.

The observed relative stability of the six-coordinate carbonyl complexes can be interpreted in view of the donating ability of the ligands involved, either the pincer or the X ligands. Concerning the pincer ligands, Brookhart has explained the lower tendency of PCP complexes to undergo reductive elimination as compared to the POCOP analogue with the generally accepted fact that phosphines are stronger σ-donors and weaker π-acceptors than phosphinites.[34] Therefore, the more electron donating PCP ligand stabilizes better an Ir(III) complex than POCOP.[66] Goldman and Krogh-Jespersen have proposed a more sophisticated interpretation of the electronic differences between the phosphine and phosphinite ligands.[67,68] On the basis of atomic orbital occupation calculations, they suggested that the overall electron density on the metal is approximately the same with both ligands (POCOP and PCP). This is because the lone pair in the backbone oxygen atoms makes the *ipso*-C atom of the aryl group of the POCOP ligand

dx.doi.org/10.1021/ic501593k | Inorg. Chem. 2014, 53, 11974−11984

more π-donating with respect to the PCP ligand, which compensates for the electron poor phosphinite donors. Calculations on the hypothetical species $[IrH_2(CO)(pincer)]$ showed that the increased π donation from the pincer backbone enhances the filled−filled π/π-interaction between the π orbital of the *ipso*-C and the filled d_{xy} orbital of the iridium. Overall, this effect destabilizes 18-electron iridium(III) complexes with respect to iridium(I) square-planar complexes (Figure 9).

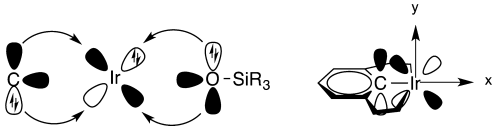

Figure 9. Filled−filled repulsive interaction between the π-system of the *ipso* carbon atom of the pincer ligand, the d_{xy} metal orbital, and the π orbital of the siloxo ligand.

In the case of siloxo complexes, the presence of the π-donating siloxo ligand causes an additional destabilizing effect, since it entertains an additional filled−filled interaction with the occupied dπ orbitals of the metal. In particular, the d_{xy} orbital is involved, which also interacts with the π-system on the *ipso* C atom (Figure 9). Caulton has studied the reaction of the 16-electron complexes $[IrH_2X(P^tBu_2Ph)_2]$ (X: Cl, Br, I, N_3, $NCNSiMe_3$, $NHC(O)CH_3$, $OC(O)CF_3$, OSO_2CF_3, $OC(O)CH_3$, SPh, OPh, F) with carbon monoxide and the tendency of the resulting carbonyl adducts to undergo HX elimination to iridium(I),[69] which was found to increase with increasing π-donation ability of the X ligand.

The present study shows that the π-donating X ligand affects the stability of the Ir(III) carbonyl complexes [IrH(X)(CO)(pincer)] (pincer = POCOP, **a**; PCP, **b**) according to the same trend of relative stability in both series **a** and **b**, but with differences that reflect the nature of these pincer ligands (see below). In the POCOP series, the Ir(III) carbonyl complexes with SBA-15 (**7a**), ^{i}Bu-POSS (**9a**), and $OSiMe_3$ (**11a**) show reductive elimination to give complex [Ir(CO)(POCOP)] (**8a**), and only the carbonyl chloride derivative **10a** is stable. Within the PCP ligand, instead, only the SBA-grafted species [IrH(O−SBA-15)(CO)(PCP)] (**7b**) undergoes reductive elimination, even if to a minimal extent, whereas the ^{i}Bu-POSS (**9b**) and chloride (**11b**) carbonyl complexes are stable and give no sign of reductive elimination.[70] Overall, our observations qualitatively confirm that iridium(III) PCP complexes have a lower tendency to give reductive elimination than their POCOP analogues. This is of paramount importance in view of the application of the iridium(III) pincer complexes **2a** and **2b** in the catalytic hydrogenation of liquid alkenes and of the connected leaching issue, which is presently under investigation.

CONCLUSIONS

Despite the different electronic properties of the POCOP and PCP ligands, the di- and tetrahydrido PCP analogues **1b** and **6b** react with the surface silanols of mesoporous silica (SBA-15) and with polysilsequioxanes according to the same pattern observed for $[IrH_2(POCOP)]$ (**1a**). The reaction of the silica grafted species **2a** and **2b** and of their soluble siloxo analogues toward carbon monoxide not only confirms the coordinatively unsaturated nature of these 16-electron species, but also indicates that PCP complexes have a lower tendency to undergo reductive elimination than their POCOP counterparts. Additionally, the NMR spectroscopic data of the siloxo complexes **2**−**5** suggest that the donating ability of the siloxo ligand influences the structure of these 16-electron species.

EXPERIMENTAL SECTION

General. NMR chemical shifts (δ) are given in ppm, and coupling constants are given in Hz. Solution NMR spectra were recorded on Bruker DPX 200, DPX 250, AVANCE III 300, AVANCE III 400, or AVANCE DPX 500 spectrometers. ^{1}H and $^{13}C\{^1H\}$ NMR chemical shifts were measured relative to the residual resonance of the deuterated solvent. The signal of the residual protio methyl group of *p*-xylene-d_{10} was set at δ 2.296 in the ^{1}H NMR and at δ 20.90 in the $^{13}C\{^1H\}$ NMR spectrum. $^{31}P\{^1H\}$ NMR spectra were referenced to external 85% H_3PO_4. Solid-state ^{1}H MAS, ^{13}C CP MAS, and ^{31}P MAS NMR spectra were recorded on a Bruker AVANCE I 400 with a conventional double resonance 2.5 mm probe head or a conventional triple resonance 4 mm probe head in double resonance mode. The samples were filled in a glovebox into a zirconia rotor and tightly closed. The spinning frequency was set at 20.00 kHz with the 2.5 mm rotor and 8.00 kHz or 10.00 kHz with the 4 mm rotor. Chemical shifts are referenced to adamantane for ^{13}C, to $(NH_4)H_2PO_4$ for ^{31}P, and to Q8M8 for ^{29}Si. ^{1}H MAS NMR spectra were obtained subtracting the background spectrum measured with an empty rotor, and the baseline was corrected. All other ^{1}H, ^{31}P spectra were baseline-corrected. FT IR spectra were recorded on a Nicolet 6700, equipped with CsI optics, collecting 16 scans at a resolution of 4 cm^{-1}. The spectra were acquired in absorbance, and baseline corrected, and no other corrections were applied. The 7 mm pellets were pressed in a glovebox (self-supported pellets for grafted compounds or CsI pellets for molecular compounds) and introduced in a 10 cm gastight cell with KBr windows. Spectra were measured between 4000 and 1400 cm^{-1} for grafted materials and between 4000 and 400 cm^{-1} for molecular species. C and H analyses were performed at the Micro-Laboratory of the Laboratory of Organic Chemistry, ETH Zurich. Carbon, phosphorus, and iridium elemental analyses of **2b** were performed at the Mikroanalytisches Labor Pascher, Remagen (Germany). Complexes $[IrH_2(POCOP)]$ (**1a**),[8] [IrH(O−SBA-15)(POCOP)] (**2a**),[9] $[IrH(OSiMe_3)(POCOP)]$ (**4a**),[9] [IrClH(POCOP)] (**5a**),[32] and [Ir(CO)(POCOP)] (**8a**)[8] were prepared according to literature procedures. $[IrH_4(PCP)]$ (**6b**) and [IrClH(PCP)] (**5b**) were prepared adapting a reported procedure (see Supporting Information). The syntheses of [IrClH(CO)(POCOP)] (**10a**), the observation of dihydrogen evolution during the synthesis of **3a**, and the detailed characterization of all the compounds are described in the Supporting Information.

[IrH($OSi_8O_{12}{}^iBu_7$)(POCOP)] (3a). $[IrH_2(POCOP)]$ (**1a**) (10 mg, 16.9 μmol), 2-butyl-POSS-monosilanol ($HOSi_8O_{12}{}^iBu_7$, 14 mg, 16.8 μmol), and toluene (4 mL) were introduced under argon atmosphere in a 20 mL Young Schlenk tube, and the resulting solution was heated at 80 °C for 5 h under static vacuum, whereupon the solution color changed from red to orange. The $^{31}P\{^1H\}$ NMR spectrum showed the quantitative consumption of the starting material **1a** and the formation of the title compound as the only P-containing product. Removal of the solvent under vacuum gave a red solid. ^{1}H NMR (500 MHz, toluene-d_8, RT): δ 6.78 (m, 1H, arom), 6.67 (m, 2H, arom), 2.15 (m, $-OCH_2CH(CH_3)_2$), 1.38 (m, 36H, ^{t}Bu), 1.16 (m, 36H, $-OCH_2CH(CH_3)_2$), 1.13 (d, J = 6.7, 6H, $-OCH_2CH(CH_3)_2$), 0.90 (d, J =6.8, 6H, $-OCH_2CH(CH_3)_2$), 0.84 (m, 8H, $-OCH_2CH(CH_3)_2$), −38.92 (t, J = 13.1, 1H, Ir−*H*). $^{31}P\{^1H\}$ NMR (202 MHz, toluene-d_8, RT): δ 170.48 (s). $^{13}C\{^1H\}$ NMR (125 MHz, toluene-d_8, RT): δ 168.0 (t, J = 5.6, 2C, *C*−O arom), 124.9 (s, C−H arom), 111.9 (br s, C arom), 105.1 (t, J = 5.0, C−H arom), 42.5 (t, J = 10.9, 2C, C_q, $C(CH_3)_3$), 39.9 (t, J = 12.6, 2C, C_q, $C(CH_3)_3$), 28.0 (t, J = 3.1, 6C, $C(CH_3)_3$), 27.9 (t, J = 3.2, 6C, $C(CH_3)_3$), 26.3 (s, 6C, $CH_2CH(CH_3)_2$), 26.1 (s, 6C, $CH_2CH(CH_3)_2$), 26.0 (s, 2C, $CH_2CH(CH_3)_2$), 24.6 (s, 3C, $CH_2CH(CH_3)_2$), 24.6 (s, 1C, $CH_2CH(CH_3)_2$), 24.5 (s, 3C, $CH_2CH(CH_3)_2$), 23.9 (s, 3C, $CH_2CH(CH_3)_2$), 23.3 (s, 3C, $CH_2CH(CH_3)_2$), 23.2 (s, 1C, $CH_2CH(CH_3)_2$). Characteristic NMR

dx.doi.org/10.1021/ic501593k | Inorg. Chem. 2014, 53, 11974−11984

data in *p*-xylene-d_{10} follow. $^{31}P\{^1H\}$ NMR (81 MHz, *p*-xylene-d_{10}, RT): δ 170.2 (s). ^1H NMR (400 MHz, *p*-xylene-d_{10}, RT): δ − 38.8 (t, J = 13.1, 1H, Ir−*H*). Anal. Calcd for $C_{15}H_{103}IrO_{15}P_2Si_8$: C = 42.20%, H = 7.30%. Found: C = 42.13%, H = 7.48%.

[IrH(O−SBA-15)(PCP)] (2b). In a typical procedure, SBA-$15_{(400)}$ (dehydroxylated at 10^{-5} mbar) (90 mg) was introduced in a 20 mL Young Schlenk tube, a pentane solution (8 mL) of [IrH_4(PCP)] (**6b**) (19 mg, 32 μmol) was added thereto, and the resulting slurry was stirred at room temperature for 1 h. The solid (approximately 91% yield) was recovered by filtration on a glass filter, washed with pentane, dried in vacuum for 12 h, and stored in a glovebox under argon. ^1H MAS NMR: δ −40.5 (Ir−*H*). ^{31}P MAS NMR: δ 66.5. ^{13}C CP-MAS NMR: δ 151 (*C*−CH_2, 2C arom), 134 (broad, *C*−Ir, 1C arom), 120 (overlapping signals, *C*−H, 3C arom), 35 (overlapping signals, CH_2 and CCH_3, 2C and 4C), 29 (CH_3, 12 C). Anal. Found (two independent determinations per each element): C = 2.30%, 2.35%; P = 0.41%, 0.42%; Ir = 1.38%, 1.39%. Averaging these data gives a loading of 4.3% w/w and a P:C:Ir mole ratio of 1:14.4:0.53 (calcd: 1:12:0.5).

[IrH($OSi_8O_{12}{}^iBu_7$)(PCP)] (3b). In a typical procedure, [IrH_4(PCP)] (**6b**) (12.2 mg, 21 μmol) was introduced in a 20 mL Young Schlenk tube and heated at 90 °C in vacuum for 3 h to generate the corresponding dihydride complex. Then, 2-butyl-POSS-monosilanol ($HOSi_8O_{12}{}^iBu_7$, 17.9 mg, 21.5 μmol) and toluene (5 mL) were added under argon. The reaction solution was heated at 80 °C for 3 h under reduced pressure, during which the completion of the reaction was monitored by $^{31}P\{^1H\}$ NMR spectroscopy. Removal of the solvent under vacuum gave a red solid. ^1H NMR (500 MHz, toluene-d_8, RT): δ 6.95 (m, 2H, arom), 6.89 (m, 1H, arom), 3.08 (dt, J = 17.6 Hz, 3.9 Hz, 2H, P−CH_2), 2.91 (dt, J = 17.5 Hz, 3.9 Hz, 2H, P−CH_2), 2.18 (m, 7H, −$OCH_2CH(CH_3)_2$), 1.34 (m, 36H, $C(CH_3)_3$), 1.18 (m, 36H, −$OCH_2CH(CH_3)_2$), 1.13 (d, J = 6.6, 6H, −$OCH_2CH(CH_3)_2$), 0.90 (d, J =7.2, 6H, −$OCH_2CH(CH_3)_2$), 0.86 (m, 8H, −$OCH_2CH(CH_3)_2$), −39.57 (t, J = 12.9, 1H, Ir−*H*). $^{31}P\{^1H\}$ NMR (202 MHz, toluene-d_8, RT): δ 64.4 (s). $^{13}C\{^1H\}$ NMR (125 MHz, toluene-d_8, RT): δ 151.6 (t, J = 7.5, 2C, *C*−CH_2 arom), 136.9 (d, J = 5.3, 1C, C arom), 122.2 (s, C−H arom), 121.2 (t, J = 7.3, C−H arom), 36.9 (t, J = 9.6, 2C, $C(CH_3)_3$), 35.3 (t, J = 14.6, 2C, CCH_2), 33.9 (t, J = 10.9, 2C, $C(CH_3)_3$), 30.2 (t, J = 2.7, 6C, $C(CH_3)_3$), 29.7 (t, J = 2.9, 6C, $C(CH_3)_3$), 26.3 (s, 6C, $CH_2CH(CH_3)_2$), 26.2 (s, 6C, $CH_2CH(CH_3)_2$), 26.0 (s, 2C, $CH_2CH(CH_3)_2$), 24.6 (m, 7C, $CH_2CH(CH_3)_2$), 24.0 (s, 3C, $CH_2CH(CH_3)_2$), 23.4 (s, 3C, $CH_2CH(CH_3)_2$), 23.2 (s, 1C, $CH_2CH(CH_3)_2$). Anal. Calcd for $C_{52}H_{107}IrO_{13}P_2Si_8$: C = 44.01%, H = 7.60%. Found: C = 43.92%, H = 7.79%.

Reaction of [IrH(O−SBA-15)(POCOP)] (2a) with CO. In a typical procedure, **2a** (115 mg) was introduced into a 20 mL Young Schlenk tube equipped with a Teflon-coated stirring bar. The Schlenk tube was evacuated and filled with carbon monoxide (1.5 bar absolute) at room temperature under stirring. The orange solid turned white instantaneously, and yellow with time (Supporting Information Figure S38). After 12 h under carbon monoxide, the Schlenk tube was evacuated and filled with argon. The ^{31}P solid-state NMR spectrum indicate the presence of [IrH(O−SBA-15)(CO)(POCOP)] (**7a**) and of [Ir(CO)(POCOP)] physisorbed on SBA-15 (**8a**). Characteristic NMR data for **7a**: ^{31}P NMR, δ 159; ^1H NMR, (Ir−*H*) δ −7.5. For **8a**: ^{31}P NMR, δ 198.

Observation of [IrH($OSi_8O_{12}{}^iBu_7$)(CO)(POCOP)] (9a). Complex **3a** (10.9 mg) was introduced in a Young NMR tube and dissolved in toluene-d_8 (0.6 mL) under argon. The NMR tube was evacuated and then filled with carbon monoxide (0.2 bar abs), whereupon the color of the solution changed from orange to pale yellow within seconds. The tube was then evacuated and filled with argon (1 bar abs). The $^{31}P\{^1H\}$ NMR spectrum of the solution showed that the starting material had reacted completely to give the Ir(III) carbonyl complex [IrH(^{i}Bu-POSS)(CO)(POCOP)] (**9a**) (δ 159.7, s, toluene-d_8) as the only P-containing product. The ^1H NMR spectrum shows a hydride signal at δ −7.04 (toluene-d_8). Upon standing in solution at room temperature, the Ir(III) carbonyl complex **9a** evolves to [Ir(CO)-(POCOP)] (**8a**) within 1 day (Supporting Information Figure S42), as indicated by the appearance of its characteristic signal at δ 198 (by literature comparison).[8] Characteristic NMR data of **9a** follow. ^1H NMR (400 MHz, toluene-d_8, RT): δ 6.73 (*m*, 1H, arom), 6.55 (*m*, 2H, arom), 1.54 (*t*, J = 7.2, 18H, ^{t}Bu) 1.39 (*t*, J = 7.2, 18H, ^{t}Bu), −7.04 (*t*, J = 16.3, 1H, Ir−*H*). $^{31}P\{^1H\}$ NMR (161 MHz, *p*-xylene-d_{10}, RT): δ 159.7 (s).

Observation of [IrH(O−SBA-15)(CO)(PCP)] (7b). [IrH(O−SBA-15)(PCP)] (**2b**) (53 mg, complex loading of approximately 17% w/w) was introduced in a 20 mL Young Schlenk tube, which was then evacuated and filled with carbon monoxide (1.2 bar abs) at room temperature. The orange solid turned instantaneously white, and the Schlenk tube was then evacuated and filled with argon. The ^{31}P MAS NMR spectra acquired within 4 h indicated the complete conversion of the starting material to the title compound **7b**. Characteristic NMR data follow for **7b**: ^{31}P MAS NMR, δ 57.3; ^1H NMR, (Ir−*H*) δ −6.9. For **8b**: ^{31}P MAS NMR, δ 81.0.

[IrH($OSi_8H_{12}{}^iBu_7$)(CO)(PCP)] (9b). [IrH($OSi_8H_{12}{}^iBu_7$)(PCP)] (**3b**) (22.2 mg, 15.7 μmol) was introduced in a 20 mL Young Schlenk tube and dissolved in toluene (6 mL) under argon. The Schlenk was evacuated and filled with carbon monoxide at 1 bar abs. Upon stirring, the solution turned light yellow immediately, and the ^1H and $^{31}P\{^1H\}$ NMR spectra indicated the quantitative formation of the title compound **9b**. Removal of the solvent under vacuum gave a yellow solid. ^1H NMR (500 MHz, toluene-d_8, RT): δ 6.9 (m, 1H, arom), 6.8 (m, 2H, arom), 2.95 (m, 4H, C−CH_2), 2.18 (m, 7H, −$OCH_2CH(CH_3)_2$), 1.46 (t, J = 6.8, 18H, $C(CH_3)_3$), 1.28 (t, J = 6.8 18H, −$OCH_2CH(CH_3)_2$), 1.18 (m, 36H, −$OCH_2CH(CH_3)_2$), 1.12 (d, J = 6.6, 6H, −$OCH_2CH(CH_3)_2$), 0.90 (d, J =7.0, 6H, −$OCH_2CH(CH_3)_2$), 0.87 (d, J = 7.0, 6H, −$OCH_2CH(CH_3)_2$), 0.83 (d, J = 7.0, 2H, −$OCH_2CH(CH_3)_2$), −6.26 (t, J = 15.0, 1H, Ir−*H*). $^{31}P\{^1H\}$ NMR (202 MHz, toluene-d_8, RT): δ 56.9 (s). $^{13}C\{^1H\}$ NMR (125 MHz, toluene-d_8, RT): δ 183.2 (br s, 1C, Ir−CO), 147.0 (t, J = 5.7, 2C, *C*−CH_2 arom), 133.7 (s, 1C, C arom), 123.6 (s, 1C, C−H arom), 121.6 (t, J = 7.0, 2C, C−H arom), 37.3 (t, J = 14.2, 2C, P−CH_2), 36.1 (t, J = 12.8, 2C, $C(CH_3)_3$), 35.4 (t, J = 9.6, 2C, $C(CH_3)_3$), 30.1 (t, J = 2.3, 6C, $C(CH_3)_3$), 29.3 (t, J = 2.0, 6C, $C(CH_3)_3$), 26.3 (s, 6C, $CH_2CH(CH_3)_2$), 26.2 (s, 6C, $CH_2CH(CH_3)_2$), 26.0 (s, 2C, $CH_2CH(CH_3)_2$), 24.6 (s, 3C, $CH_2CH(CH_3)_2$), 24.6 (s, 3C, $CH_2CH(CH_3)_2$), 24.6 (s, 1C, $CH_2CH(CH_3)_2$), 24.0 (s, 3C, $CH_2CH(CH_3)_2$), 23.4 (s, 3C, $CH_2CH(CH_3)_2$), 23.2 (s, 1C, $CH_2CH(CH_3)_2$). Anal. Calcd for $C_{53}H_{107}IrO_{14}P_2Si_8$: C = 43.99%, H = 7.45%. Found: C = 43.97%, H = 7.38%.

■ ASSOCIATED CONTENT

Ⓢ Supporting Information

Complete experimental procedures, and NMR and IR spectra. This material is available free of charge via the Internet at http://pubs.acs.org.

■ AUTHOR INFORMATION

Corresponding Author

*E-mail: mezzetti@inorg.chem.ethz.ch.

Notes

The authors declare no competing financial interest.

■ ACKNOWLEDGMENTS

We thank Prof. Jeroen A. van Bokhoven for discussion, Dr. René Verel for NMR spectroscopic assistance, Mr. Daniel Fodor for preparing some of the SBA samples, and Mr. Karol Furman for performing nitrogen physisorption measurements.

■ REFERENCES

(1) Maschmeyer, T.; Rey, F.; Sankar, G.; Thomas, J. M. *Nature* **1995**, *378*, 159.

(2) Anwander, R. *Chem. Mater.* **2001**, *13*, 4419.

(3) Buffon, R.; Rinaldi, R. In *Modern Surface Organometallic Chemistry*; Basset, J. M., Psaro, R., Roberto, D., Ugo, R., Eds.; Wiley-VCH: Weinheim, 2009; p 417.

(4) *Design and Application of Single-Site Heterogeneous Catalysts*; Thomas, J. M., Ed.; Imperial College Press: London, 2012.
(5) Rimoldi, M.; Mezzetti, A. *Catal. Sci. Technol.* **2014**, *4*, 2724.
(6) Foley, H. C.; DeCanio, S. J.; Tau, K. D.; Chao, K. J.; Onuferko, J. H.; Dybowski, C.; Gates, B. C. *J. Am. Chem. Soc.* **1983**, *105*, 3074.
(7) Lu, J.; Aydin, C.; Browning, N. D.; Gates, B. C. *J. Am. Chem. Soc.* **2012**, *134*, 5022.
(8) Gottker-Schnetmann, I.; White, P. S.; Brookhart, M. *Organometallics* **2004**, *23*, 1766.
(9) Rimoldi, M.; Fodor, D.; van Bokhoven, J. A.; Mezzetti, A. *Chem. Commun.* **2013**, *49*, 11314.
(10) Averseng, F.; Vennat, M.; Che, M. In *Handbook of Heterogeneous Catalysis*; Ertl, G., Knözinger, H., Schüth, F., Weitkamp, J., Eds.; Wiley-VCH: Weinheim, 2008; p 522.
(11) Scott, S. L.; Szpakowicz, M.; Mills, A.; Santini, C. C. *J. Am. Chem. Soc.* **1998**, *120*, 1883.
(12) Richmond, M. K.; Scott, S. L.; Alper, H. *J. Am. Chem. Soc.* **2001**, *123*, 10521.
(13) Bonati, M. L. M.; Douglas, T. M.; Gaemers, S.; Guo, N. *Organometallics* **2012**, *31*, 5243.
(14) Huang, E. K.; Cheung, W. M.; Chan, K. W.; Lam, F. L. Y.; Hu, X. J.; Zhang, Q. F.; Williams, I. D.; Leung, W. H. *Eur. J. Inorg. Chem.* **2013**, *2013*, 2893.
(15) Ward, M. D.; Harris, T. V.; Schwartz, J. *J. Chem. Soc., Chem. Commun.* **1980**, 357.
(16) Trovitch, R. J.; Guo, N.; Janicke, M. T.; Li, H.; Marshall, C. L.; Miller, J. T.; Sattelberger, A. P.; John, K. D.; Baker, R. T. *Inorg. Chem.* **2010**, *49*, 2247.
(17) Liang, Y.; Anwander, R. *Dalton Trans.* **2013**, *42*, 12521.
(18) Nozaki, C.; Lugmair, C. G.; Bell, A. T.; Tilley, T. D. *J. Am. Chem. Soc.* **2002**, *124*, 13194.
(19) Ruddy, D. A.; Jarupatrakorn, J.; Rioux, R. M.; Miller, J. T.; McMurdo, M. J.; McBee, J. L.; Tupper, K. A.; Tilley, T. D. *Chem. Mater.* **2008**, *20*, 6517.
(20) Marciniec, B.; Szubert, K.; Potrzebowski, M. J.; Kownacki, I.; Łęszczak, K. *Angew. Chem., Int. Ed.* **2008**, *47*, 541.
(21) Silvennoinen, R. J.; Jylhä, O. J. T.; Lindblad, M.; Sainio, J. P.; Puurunen, R. L.; Krause, A. O. I. *Appl. Surf. Sci.* **2007**, *253*, 4103.
(22) Meyer, T. Y.; Woerpel, K. A.; Novak, B. M.; Bergman, R. G. *J. Am. Chem. Soc.* **1994**, *116*, 10290.
(23) Kaplan, A. W.; Bergman, R. G. *Organometallics* **1998**, *17*, 5072.
(24) Zhao, D.; Feng, J.; Huo, Q.; Melosh, N.; Fredrickson, G. H.; Chmelka, B. F.; Stucky, G. D. *Science* **1998**, *279*, 548.
(25) Zhao, D.; Huo, Q.; Feng, J.; Chmelka, B. F.; Stucky, G. D. *J. Am. Chem. Soc.* **1998**, *120*, 6024.
(26) Dufour, P.; Scott, S. L.; Santini, C. C.; Lefebvre, F.; Basset, J.-M. *Inorg. Chem.* **1994**, *33*, 2509.
(27) Feher, F. J.; Newman, D. A.; Walzer, J. F. *J. Am. Chem. Soc.* **1989**, *111*, 1741.
(28) Abbenhuis, H. C. L. *Chem.—Eur. J.* **2000**, *6*, 25.
(29) Duchateau, R. *Chem. Rev.* **2002**, *102*, 3525.
(30) Cordes, D. B.; Lickiss, P. D.; Rataboul, F. *Chem. Rev.* **2010**, *110*, 2081.
(31) Quadrelli, E. A.; Basset, J.-M. *Coord. Chem. Rev.* **2010**, *254*, 707.
(32) Gottker-Schnetmann, I.; White, P.; Brookhart, M. *J. Am. Chem. Soc.* **2004**, *126*, 1804.
(33) Kanzelberger, M.; Zhang, X.; Emge, T. J.; Goldman, A. S.; Zhao, J.; Incarvito, C.; Hartwig, J. F. *J. Am. Chem. Soc.* **2003**, *125*, 13644.
(34) Sykes, A. C.; White, P.; Brookhart, M. *Organometallics* **2006**, *25*, 1664.
(35) Choi, J.; Choliy, Y.; Zhang, X.; Emge, T. J.; Krogh-Jespersen, K.; Goldman, A. S. *J. Am. Chem. Soc.* **2009**, *131*, 15627.
(36) Zhang, X. W.; Emge, T. J.; Ghosh, R.; Krogh-Jespersen, K.; Goldman, A. S. *Organometallics* **2006**, *25*, 1303.
(37) Moulton, C. J.; Shaw, B. L. *J. Chem. Soc., Dalton Trans.* **1976**, 1020.
(38) Morales-Morales, D.; Lee, D. W.; Wang, Z.; Jensen, C. M. *Organometallics* **2001**, *20*, 1144.
(39) Looney, A.; Han, R.; Gorrell, I. B.; Cornebise, M.; Yoon, K.; Parkin, G.; Rheingold, A. L. *Organometallics* **1995**, *14*, 274.
(40) Veith, M.; Vogelgesang, H.; Huch, V. *Organometallics* **2002**, *21*, 380.
(41) Veith, M.; Frères, J.; Huch, V.; Zimmer, M. *Organometallics* **2006**, *25*, 1875.
(42) Nedez, C.; Choplin, A.; Lefebvre, F.; Basset, J. M.; Benazzi, E. *Inorg. Chem.* **1994**, *33*, 1099.
(43) Nedez, C.; Theolier, A.; Lefebvre, F.; Choplin, A.; Basset, J. M.; Joly, J. F. *J. Am. Chem. Soc.* **1993**, *115*, 722.
(44) He, M. Y.; Xiong, G.; Toscano, P. J.; Burwell, R. L.; Marks, T. J. *J. Am. Chem. Soc.* **1985**, *107*, 641.
(45) Marciniec, B.; Maciejewski, H. *Coord. Chem. Rev.* **2001**, *223*, 301.
(46) Kownacki, I.; Kubicki, M.; Marciniec, B. *Inorg. Chim. Acta* **2002**, *334*, 301.
(47) Kownacki, I.; Kubicki, M.; Szubert, K.; Marciniec, B. *J. Organomet. Chem.* **2008**, *693*, 321.
(48) Zhang, F.; Wang, L.; Chang, S.-H.; Huang, K.-L.; Chi, Y.; Hung, W.-Y.; Chen, C.-M.; Lee, G.-H.; Chou, P.-T. *Dalton Trans.* **2013**, *42*, 7111.
(49) Schmidbaur, H.; Adlkofer, J. *Chem. Ber.* **1974**, *107*, 3680.
(50) Kownacki, I.; Marciniec, B.; Szubert, K.; Kubicki, M. *Organometallics* **2005**, *24*, 6179.
(51) Marciniec, B.; Kownacki, I.; Kubicki, M. *Organometallics* **2002**, *21*, 3263.
(52) Truscott, B. J.; Nelson, D. J.; Lujan, C.; Slawin, A. M. Z.; Nolan, S. P. *Chem.—Eur. J.* **2013**, *19*, 7904.
(53) Wolczanski, P. T. *Polyhedron* **1995**, *14*, 3335.
(54) Poulton, J. T.; Folting, K.; Streib, W. E.; Caulton, K. G. *Inorg. Chem.* **1992**, *31*, 3190.
(55) Poulton, J. T.; Sigalas, M. P.; Folting, K.; Streib, W. E.; Eisenstein, O.; Caulton, K. G. *Inorg. Chem.* **1994**, *33*, 1476.
(56) Although the effect of electron density in ^{13}C NMR chemical shift is relatively small compared to that in ^{1}H NMR spectrum, $\Delta\delta$ can still be appreciated.
(57) Riehl, J. F.; Jean, Y.; Eisenstein, O.; Pelissier, M. *Organometallics* **1992**, *11*, 729.
(58) Mayer, J. M. *Comments Inorg. Chem.* **1988**, *8*, 125.
(59) Caulton, K. G. *New J. Chem.* **1994**, *18*, 25.
(60) Punji, B.; Emge, T. J.; Goldman, A. S. *Organometallics* **2010**, *29*, 2702.
(61) Jean, Y.; Eisenstein, O. *Polyhedron* **1988**, *7*, 405.
(62) Rachidi, I. E.; Eisenstein, O.; Jean, Y. *New J. Chem.* **1990**, *14*, 671.
(63) Small shifts in the ν(CO) stretching frequency have been observed for metal carbonyl complexes physisorbed on silica, see for instance: (a) Serp, P.; Kalck, P.; Feurer, R. *Chem. Rev.* **2002**, *102*, 3085. (b) Shephard, D. S.; Maschmeyer, T.; Johnson, B. F. G.; Thomas, J. M.; Sankar, G.; Ozkaya, D.; Zhou, W.; Oldroyd, R. D.; Bell, R. G. *Angew. Chem., Int. Ed.* **1997**, *36*, 2242. Interestingly, the physisorbed complex **8a** shows stronger interactions with the silica surface than the grafted species **7a** (see Supporting Information, page S23).
(64) The ^{31}P NMR chemical shifts mainly depend on the Ir−P bond distance (and related angles), and thus on first-coordination-sphere effects.
(65) Segawa, Y.; Yamashita, M.; Nozaki, K. *J. Am. Chem. Soc.* **2009**, *131*, 9201.
(66) The interpretation of Brookhart refers to the five-coordinated complex [IrH(NHPh)(POCOP)] and its tendency to give the related Ir(I) species [Ir(NH_2Ph)(POCOP)] with respect to [IrH(NHPh)-(PCP)] that is stable only in the Ir(III) oxidation state (see ref 34). Here, similarly, our discussion concerns the reductive elimination of six-coordinated Ir(III) carbonyl complexes [IrH(OSi)(CO)(pincer)] (pincer POCOP, PCP) to eliminate a silanol, resulting in the Ir(I) carbonyl complex [Ir(CO)(pincer)].
(67) Krogh-Jespersen, K.; Czerw, M.; Zhu, K.; Singh, B.; Kanzelberger, M.; Darji, N.; Achord, P. D.; Renkema, K. B.; Goldman, A. S. *J. Am. Chem. Soc.* **2002**, *124*, 10797.

(68) Zhu, K.; Achord, P. D.; Zhang, X.; Krogh-Jespersen, K.; Goldman, A. S. *J. Am. Chem. Soc.* **2004**, *126*, 13044.
(69) Cooper, A. C.; Bollinger, J. C.; Huffman, J. C.; Caulton, K. G. *New J. Chem.* **1998**, *22*, 473.
(70) The different behavior of the SBA-15 and ^{i}Bu-POSS derivatives in the PCP series deserves future attention in view of the applicability of polysilsequioxane as models for the silica surface.